PLATE MODE VELOCITIES IN GRAPHITE/EPOXY PLATES

W. H. Prosser and M. R. Gorman*
MS 231
NASA Langley Research Center
Hampton, VA 23665
(804) 864-4960

*Dept. of Engineering
University of Denver
Denver, CO 80208-0177
(303) 871-2102

Submitted for publication to the Journal of the Acoustical Society of America
10 June 1993

ABSTRACT

Measurements of the velocities of the extensional and flexural plate modes were made along three directions of propagation in four graphite/epoxy composite plates. The acoustic signals were generated by simulated acoustic emission events (pencil lead breaks or Hsu-Neilsen sources) and detected by broad band ultrasonic transducers. The first arrival of the extensional plate mode, which is nondispersive at low frequencies, was measured at a number of different distances from the source along the propagation direction of interest. The velocity was determined by plotting the distance versus arrival time and computing its slope. Because of the large dispersion of the flexural mode, a Fourier phase velocity technique was used to characterize this mode. The velocity was measured up to a frequency of 160 kHz. Theoretical predictions of the velocities of these modes were also made and compared with experimental observations. Classical plate theory yielded good agreement with the measured extensional velocities. For predictions of the dispersion of the flexural mode, Mindlin plate theory, which includes the effects of shear deformation and rotatory inertia was shown to give better agreement with the experimental measurements.

INTRODUCTION

Acoustic signals propagate in thin plates as the extensional and flexural plate modes when the wavelength of the acoustic signal is much larger than the plate thickness. This fact is of importance in a number of nondestructive evaluation (NDE) techniques that use acoustic waves such as the acoustic emission (AE) technique. The propagation of AE signals as plate modes has been demonstrated by a number of researchers. It was shown using simulated AE sources (pencil lead breaks) by Gorman [1] on thin aluminum and gr/ep composite plates and by Gorman and Prosser [2] on thin aluminum plates. A typical signal from a simulated AE source (pencil lead break) which identifies these two modes is shown in Figure 1. The extensional and flexural mode components of this waveform are identified in this figure. AE signals from transverse matrix cracking sources in gr/ep composite plates were also shown to propagate as plate modes by Gorman and Ziola [3]. Smith [4] showed that crack growth events in thin aluminum plates under spectrum fatigue loading produced signals that propagated as plate modes.

The propagation of acoustic signals as plate modes in thin plates also occurs in other NDE techniques such as conventional ultrasonic testing, acousto-ultrasonics, and laser generated ultrasonics. Duke et al. [5] suggested that the acousto-ultrasonic technique generated plate modes, made tone burst measurements of the velocities of the plate modes, and compared them with predictions based on classical plate theory (CPT). Schumacher et al. [6] demonstrated the existence of plate modes in laser generated ultrasonic signals in thin plates which were detected by noncontacting laser interferometers. They also made measurements of the dispersion of these two modes in steel plates and compared them with theory and finite element modelling.

For all of these NDE techniques, the propagation characteristics of these plate modes are of great importance. In acoustic emission testing, Gorman [1] discussed how erroneous source location could be obtained using conventional first threshold crossing or peak arrival techniques because of the presence of plate modes which propagate with different and dispersive velocities. Such source location errors were substantiated by Ziola and Gorman [7] and an alternative method for source location based on

cross-correlation of the flexural mode waves was demonstrated. In the other mentioned NDE techniques, measurements of the velocities of the plate modes are useful for determining material properties and locating flaws. Mal et al. [8], Veidt and Sayir [9], and Dean [10] have discussed how measurements of flexural mode dispersion might be useful in determining the elastic constants of composite plates.

In this research, measurements were made of the extensional and flexural plate mode velocities on four different composite laminates in three directions of propagation. The ply layups for these laminates were $[0_{16}]$, $[0_4,90_4]_s$, $[0,90]_{4s}$, and $[0,45,-45,90]_{2s}$. Pencil lead breaks (Hsu-Neilsen sources) were used to generate the acoustic signals which were detected by wide band ultrasonic sensors. The first arrival time of the extensional mode as a function of distance from the source was used to compute its velocity. A Fourier phase technique was used to determine the flexural mode dispersion up to a frequency of 160 kHz. The measurements were made along the two principal axes (0 and 90 degrees) in the plane of the plate and at an angle of 45 degrees.

The ability of existing plate theories for predicting the measured plate mode velocities was also investigated. Classical plate theory (CPT) was successfully used to predict the velocity of the extensional plate mode using elastic moduli calculated from laminated plate theory. The experimentally measured flexural mode dispersion curves were also compared with theoretical predictions based on CPT. The lack of agreement between theory and experiment at the higher frequencies demonstrated the limitations of CPT for composite materials. These are caused by the effects of shear deformation and rotatory inertia which are neglected in CPT. Mindlin plate theory which includes these effects was then used to predict the dispersion behavior for this mode. These predictions were in much better agreement with the experimental flexural mode dispersion measurements.

I THEORY

In this research, two theoretical approaches were used for predicting the behavior of plate mode waves in gr/ep composite laminates. The first theoretical predictions were based on classical plate theory (CPT). This is a widely used approximate theory for describing motion in thin plates where the wavelength (λ) is much larger than the plate thickness (h). A number of authors have presented CPT in detail including Graff [11] who

derives the equations of motion for isotropic materials and Whitney [12] who includes the effects of anisotropy. For extensional mode waves in a symmetric orthotropic laminate, the predictions of the velocity are derived from the equations of motion for in-plane displacements which are given by

$$A_{11}\frac{\partial^2 u_0}{\partial x^2} + A_{66}\frac{\partial^2 u_0}{\partial y^2} + (A_{12} + A_{66})\frac{\partial^2 v_0}{\partial x \partial y} = \rho h \frac{\partial^2 u_0}{\partial t^2} \qquad \text{Eq. 1}$$

and

$$A_{22}\frac{\partial^2 v_0}{\partial y^2} + A_{66}\frac{\partial^2 v_0}{\partial x^2} + (A_{12} + A_{66})\frac{\partial^2 u_0}{\partial x \partial y} = \rho h \frac{\partial^2 v_0}{\partial t^2} \quad . \qquad \text{Eq. 2}$$

In the previous equations, u_0 and v_0 are the midplane displacements along the x and y axes which are orthogonal axes in the plane of the plate, ρ is the density, and the A_{ij}'s are the anisotropic in-plane stiffness coefficients obtained from laminated plate theory as described by Whitney [12] or Tsai and Hahn [13].

These equations predict two modes of propagation. In general, one mode is quasi-extensional with the largest component of its particle displacement along the propagation direction and the other is quasi-in-plane shear with the largest component of particle displacement perpendicular to the direction of propagation in the plane of the plate. Along symmetry directions, these modes are pure mode extensional and shear-horizontal (SH) plate modes. The dispersion relations for these two waves are determined by substituting a plane wave displacement into the equations of motion and solving the resulting Christoffel's equation. For propagation along the x axis or 0 degree direction, this procedure produces an extensional mode that is pure mode and whose velocity (c_e) is given by

$$c_e = \sqrt{\frac{A_{11}}{\rho h}} \quad . \qquad \text{Eq. 3}$$

Along the y axis, the extensional mode is also pure mode and its velocity is given by

$$c_e = \sqrt{\frac{A_{22}}{\rho h}} \quad . \qquad \text{Eq. 4}$$

For propagation at 45 degrees between x and y, the wave is quasi-extensional with a velocity given by

$$c_e = \sqrt{\frac{(A_{11} + 2A_{66} + A_{22}) + \sqrt{R}}{4\rho h}} \qquad \text{Eq. 5}$$

where

$$R = (A_{11} + 2A_{66} + A_{22})^2 - 4(A_{11} + A_{66})(A_{22} + A_{66}) + 4(A_{12} + A_{66})^2 \quad . \qquad \text{Eq. 6}$$

For flexural waves, CPT was again used to predict the dispersion. In this case, the plate is assumed to be under a state of pure bending in which plane sections of the plate remain plane and perpendicular to the midplane of the plate. Thus, shear deformation is not included in this theory. A state of plane stress is assumed and the effects of rotatory inertia are also neglected. The CPT equation of motion for an orthotropic composite laminate in the absence of body forces is

$$D_{11}\frac{\partial^4 w}{\partial x^4} + 4D_{16}\frac{\partial^4 w}{\partial x^3 \partial y} + 2(D_{12} + 2D_{66})\frac{\partial^4 w}{\partial x^2 \partial y^2} + 4D_{26}\frac{\partial^4 w}{\partial x \partial y^3} + D_{22}\frac{\partial^4 w}{\partial y^4} + \rho h\frac{\partial^2 w}{\partial t^2} = 0 \qquad \text{Eq. 7}$$

where the D_{ij}'s are the anisotropic bending stiffness coefficients obtained from laminated plate theory as described by Whitney [12] or Tsai and Hahn [13]. In the previous equation, w is the displacement along the z axis which is normal to the plane of the plate.

The dispersion behavior for the flexural mode using CPT is also obtained by substituting the displacement for a plane wave propagating along the direction of interest into the equation of motion. After substitution and reduction of terms, the resulting CPT dispersion relation along the x axis is

$$c_f = \sqrt[4]{\frac{D_{11}}{\rho h}}\sqrt{\omega} \qquad \text{Eq. 8}$$

where c_f is the velocity of the flexural mode and ω is the angular frequency. Along the y axis, the dispersion relation is

$$c_f = \sqrt[4]{\frac{D_{22}}{\rho h}}\sqrt{\omega} \qquad \text{Eq. 9}$$

and at 45 degrees the dispersion relation is

$$c_f = \sqrt[4]{\frac{\frac{1}{4}\left(D_{11} + 4D_{16} + 2\left(D_{12} + 2D_{66}\right) + 4D_{26} + D_{22}\right)}{\rho h}}\sqrt{\omega} \quad . \qquad \text{Eq. 10}$$

Unlike the predictions for the extensional mode, the flexural mode is predicted to have a velocity that is dispersive. The velocity is predicted to increase as the square root of the frequency.

Although CPT yielded good results for the case of the extensional mode, it was found to be of limited value for the flexural mode because of the effects of shear deformation and rotatory inertia. Thus, a second theory was also used to predict the dispersion of the flexural mode. This theory includes the effects of shear deformation and rotatory inertia. It was put forth by Tang et al. [14] following earlier work by Yang et al [15] which was an extension of Mindlin plate theory[16]. A detailed presentation of this theory is beyond the scope of this paper. However, the dispersion behavior for a symmetric orthotropic laminate is obtained when the determinant of the following matrix of coefficients is set equal to zero

$$\begin{vmatrix} M_{11} & M_{12} & M_{13} \\ M_{21} & M_{22} & M_{23} \\ M_{31} & M_{32} & M_{33} \end{vmatrix} \qquad \text{Eq. 11}$$

where

$$M_{11} = D_{11}k^2l_x^2 + 2D_{16}k^2l_xl_y + D_{66}k^2l_y^2 + A_{55} - I\omega^2 \qquad \text{Eq. 12}$$

$$M_{12} = D_{16}k^2 + \left(D_{12} + D_{66}\right)k^2l_xl_y \qquad \text{Eq. 13}$$

$$M_{13} = iA_{55}kl_x \qquad \text{Eq. 14}$$

$$M_{21} = D_{16}k^2 + (D_{12} + D_{66})\,k^2 l_x l_y \qquad \text{Eq. 15}$$

$$M_{22} = D_{66}k^2 l_x^2 + 2D_{16}k^2 l_x l_y + D_{22}k^2 l_y^2 + A_{44} - I\omega^2 \qquad \text{Eq. 16}$$

$$M_{23} = iA_{44}kl_y \qquad \text{Eq. 17}$$

$$M_{31} = -iA_{55}kl_x \qquad \text{Eq. 18}$$

$$M_{32} = -iA_{44}kl_y \qquad \text{Eq. 19}$$

and

$$M_{33} = A_{55}k^2 l_x^2 + A_{44}k^2 l_y^2 - \rho^*\omega^2 \quad . \qquad \text{Eq. 20}$$

In the previous equations, l_x and l_y are the direction cosines for the propagation direction of interest, k is the wave number,

$$(\rho^*, I) = \int_{z=-\frac{h}{2}}^{z=\frac{h}{2}} \rho\,(1, z^2)\,dz \quad , \qquad \text{Eq. 21}$$

and

$$A_{ij} = \kappa_i \kappa_j \int_{z=-\frac{h}{2}}^{z=\frac{h}{2}} (Q_{ij})_l\,dz \qquad \text{for i,j = 4,5.} \qquad \text{Eq. 22}$$

In Eq. 22, the κ_i are shear correction factors which were determined to yield the best agreement with three dimensional elasticity theory when κ_i^2=5/6. The subscript l refers to the l'th layer of the laminate and the Q_{ij} are the stiffnesses for the l'th layer. Solving the determinant for the wavenumber as a function of ω yields a cubic in k^2. Only the root which approaches zero as the frequency approaches zero is the correct root. Once k as a function of ω is known, the phase velocity is determined as a function of frequency using the relation

$$c_f = \frac{\omega}{k} \quad . \qquad \text{Eq. 23}$$

II EXPERIMENT

The composite laminates used in this study were made of AS4/3502 graphite/epoxy. All four laminates consisted of sixteen plys and had a nominal thickness of 2.26 mm. The dimensions were 0.508 m. along the x direction (0 degree ply direction) and 0.381 m. along the y direction. Measurements were made along the 0 degree (x direction), 45, and 90 degree directions for all four laminates. The nominal lamina properties for this material as obtained from the manufacturer are given in Table I. These values were used in the laminated plate theory calculations to obtain the in-plane and bending stiffness coefficients needed for the theoretical dispersion calculations.

For measurements of the extensional and flexural velocities, a pencil lead bread was used to excite the acoustic waves. The waves were detected with Panametrics 3.5 MHz broad band ultrasonic transducers. These sensors have been shown previously by Prosser [17] to provide flat frequency, displacement sensitivity response to these low frequency plate waves. The detected signals were preamplified by 40 dB with model 1220A preamplifiers from Physical Acoustic Corporation (PAC). There were no filters used in the preamps. The amplified signals were digitized at a sampling frequency of 5 MHz for the extensional measurements and 1 MHz for the flexural measurements with a LeCroy 6810 transient recorder, and then stored on a personal computer for analysis. A high sensitivity resonant AE transducer (PAC model R15) was positioned next to the lead break and was used to trigger the transient recorder.

For the extensional measurements, a single receiving sensor was used to detect the waves along the propagation direction of interest. The simulated AE signal was repeated five times while the receiving transducer was moved over a range of distances from the source which varied from 7.62 cm. to 17.78 cm. in 2.54 cm. increments. The first arrival time of the extensional mode was then determined for each of the signals from the digitized time records and plotted as a function of distance from the source. A linear least squares fit was used to determine the slope of the curve which is the velocity of the extensional mode. This process was repeated

for each of the three directions in the four plates. A typical plot of the extensional arrival time versus distance of propagation is shown in Figure 2.

A Fourier phase technique was used for the measurement of the flexural mode dispersion. This technique has been described by a number of authors including Sachse and Pao [18], Pao and Sachse [19], Veidt and Sayir [9], Dean [10], and Alleyne and Cawley [20]. In this technique, the elastic wave is detected at two different distances away from the source of the wave along the direction of propagation of interest. The phase (φ) of the wave at each position at a given frequency (f) is determined by performing a Fourier Transform on the signals. The phase must be unwrapped to remove the $2n\pi$ uncertainty. The phase difference ($\Delta\varphi$) over the distance between the two transducers (Δx) is then computed for each frequency. The wave number and velocity are then calculated at each frequency by

$$k(f) = \frac{\Delta\varphi(f)}{\Delta x} \qquad \text{Eq. 24}$$

and

$$c(f) = \frac{2\pi f}{k(f)} = \frac{2\pi f \Delta x}{\Delta\varphi(f)} \quad . \qquad \text{Eq. 25}$$

The experimental setup used for these experiments is shown in Figure 3. Transducer separations of 1.91, 2.54, 3.18, 3.81, and 4.45 cm were used. An average velocity and standard deviation for the five different measurements was computed. The source and receivers were kept as nearly in the center of the plate as possible to minimize reflections.

Prior to computing the FFT to determine the phase, the higher frequency extensional mode and the reflections arriving later in the flexural mode were zeroed out in the computer. Previous Fourier analysis of the flexural mode signals when digitized at much higher sampling frequencies (100 MHz) showed that the maximum frequency component in the flexural mode was about 200 kHz. Thus, aliasing was not a concern even at the low sampling frequency of 1 MHz.

III RESULTS AND DISCUSSION

The measured and theoretical extensional velocities for all four lam-

inates are shown in Table II. The measured velocities were consistently lower than the predicted velocities with the exceptions of the 90 degree measurements in the $[0_{16}]$ and the $[0_4,90_4]_s$ plates and the 45 degree measurement in the $[0_{16}]$ laminate. With these exceptions, the measured velocities were all in the range of two to nine percent less than the theoretical velocities. This would seem to indicate that the manufacturer's properties used in the theoretical calculations were somewhat higher than those in the actual material. Variations in material properties are common for these materials and are due to fiber volume variations, cure processing variations, and variations in resin chemistry. The 45 degree $[0_{16}]$ measurement was much less than theoretically predicted. It is not known why this discrepancy occurred and further investigation is needed. The remaining two exceptions, propagation at 90 degrees in the $[0_{16}]$ and the $[0_4,90_4]_s$ laminates, were only slightly higher than predicted values.

The average measured flexural velocities for the 0, 45, and 90 degree directions in the $[0_{16}]$ graphite epoxy plate are plotted in Figure 4 to Figure 6 with the standard deviation of the measured values indicated by error bars. The predicted velocity dispersion curves for CPT and Mindlin plate theory are also shown in these plots. The agreement between measurement and Mindlin plate theory is excellent for the 90 degree propagation direction. For propagation at 45 and 0 degrees, the measured values are consistently less than those predicted by theory. The discrepancy at 0 and 45 degrees is consistent with the differences between theory and experiment observed for the extensional mode.

The effect of shear and rotatory inertia is clear when CPT and Mindlin plate theory are compared in these plots. They are in agreement at very low frequencies in all cases where the approximations of CPT are valid. The discrepancy increases with increasing frequency as the velocity predicted by CPT increases without bound.

It is also apparent that the difference between Mindlin plate theory and CPT is much greater for the 0 and 45 degree directions than for the 90 degree direction. This is expected since the shear modulus is much smaller in comparison to the Young's modulus in those directions. CPT is based on the assumption of no shear deformation which implies an infinite shear modulus. Thus, better agreement is provided by CPT when the ratio of the shear modulus to the Young's modulus is larger.

A plot of the measured velocities and the Mindlin plate theory predictions for the $[0,90]_{4S}$ plate is shown in Figure 7. In order to better view this complicated graph, the CPT predictions and the experimental uncertainties are not shown in the plot. In this plate, the measured velocities were less than theoretical predictions for all three directions of propagation. However, the measured and theoretical velocities occurred in the same order with the 0 degree velocity being the largest, followed next by the 90 degree velocity, and with the 45 degree velocity the smallest. The results for the other two laminates were similar with the measured velocities consistently less than predicted by theory. This again seems to indicate that the actual material properties are less than the nominal properties used in the theoretical calculations and is consistent with the extensional measurements.

In summary, the velocity of the extensional plate mode and the dispersion of the flexural plate mode was measured along three directions of propagation in four graphite/epoxy laminates. Theoretical predictions of the dispersion of these modes were made with CPT and Mindlin plate theory. CPT yielded good agreement with the extensional velocity but was shown to be of limited value in predicting the dispersion of the flexural mode because it assumes that the effects of shear deformation and rotatory inertia are negligible. Mindlin plate theory, which includes these effects, gave much better agreement with the measured flexural dispersion. However, there was a consistent discrepancy between theory and experiment believed to be due to variations in actual material properties from those used in the calculations.

REFERENCES

[1] M. R. Gorman, “Plate Wave Acoustic Emission,” Journal of the Acoustical Society of America, **90**(1) 358-364 (1990).

[2] M. R. Gorman and W. H. Prosser, “AE Source Orientation by Plate Wave Analysis,” Journal of Acoustic Emission, **9**(4) 283-288 (1990).

[3] M. R. Gorman and S. M. Ziola, “Plate Waves Produced by Transverse Matrix Cracking,” Ultrasonics, **29** 245-251 (1991).

[4] W. D. Smith, Jr., “Acoustic Emission From Spectrum Fatigue Cracks in 7075 Aluminum,” Masters Thesis, Naval Postgraduate School, (1990).

[5] J. C. Duke, Jr., E. G. Henneke II, and W. W. Stinchcomb, “Ultrasonic Stress Wave Characterization of Composite Materials,” NASA Contractor Report 3976, (1986).

[6] N. A. Schumacher, P. H. Gien, and C. P. Burger, “Analysis of Transient Lamb Waves on Metal Plates, Composite Panels and Curved Members,” Review of Progress in Quantitative NDE, **11B** 1569-1576 (1991).
[7] S. M. Ziola and M. R. Gorman, “Source Location in Thin Plates Using Cross-Correlation,” Journal of the Acoustical Society of America, **90**(5) 2551-2556 (1991).
[8] A. K. Mal, M. R. Gorman, and W. H. Prosser, “Material Characterization or Composite Laminates Using Low-Frequency Plate Wave Dispersion Data, Review of Progress in Quantitative NDE, **11B** 1451-1458 (1991).
[9] M. Veidt and M. Sayir, “Experimental Evaluation of Global Composite Laminate Stiffnesses by Structural Wave Propagation,” Journal of Composite Materials, **24** 688-706 (1990).
[10] G. D. Dean, “The Use of Plate Bending Waves for Elastic Property Determination of Polymers,” National Physical Laboratory Report DMA(A)166, (Teddington, Middlesex, UK, 1988).
[11] K. F. Graff, Wave Motion in Elastic Solids, (Universities Press, Belfast, 1975).
[12] J. W. Whitney, Structural Analysis of Laminated Anisotropic Plates, (Technomic Publishing Co., Lancaster, Pennsylvania, 1987).
[13] S. W. Tsai and H. T. Hahn, Introduction to Composite Materials, (Technomic Publishing Co., Lancaster, Pennsylvania, 1980).
[14] B. Tang, E. G. Henneke II, and R. C. Stiffler, “Low Frequency Flexural Wave Propagation in Laminated Composite Plates,” Proceedings on a Workshop on Acousto-Ultrasonics: Theory and Applications, Blacksburg Virginia, (1987) pp. 45-65.
[15] P. C. Yang, C. H. Norris, and Y. Stavsky, “Elastic Wave Propagation in Heterogeneous Plates”, International Journal of Solids and Structures, **2** 665-684 (1966).
[16] R. D. Mindlin, “Influence of Rotatory Inertia and Shear on Flexural Motions of Isotropic, Elastic Plates,” Journal of Applied Mechanics, **2** 31-38 (1951).
[17] W. H. Prosser, “The Propagation Characteristics of the Plate Modes of Acoustic Emission Waves in Thin Aluminum Plates and Thin Graphite/Epoxy Composite Plates and Tubes,” NASA Technical Memorandum 104187, (1991).
[18] W. Sachse and Y. H. Pao, “On the Determination of Phase and Group Velocities of Dispersive Waves in Solids,” Journal of Applied Physics, **49**(8) 4320-4327 (1978).
[19] Y. H. Pao and W. Sachse, “Ultrasonic Phase Spectroscopy and the Dispersion of Elastic Waves in Solids,” Proceedings of the Ninth International Congress on Acoustics, Madrid Spain, (1977) p. 734.
[20] D. Alleyne and P. Cawley, “A Two-Dimensional Fourier Transform Method for the Measurement of Propagating Multimode Signals,” Journal of the Acoustical Society of America, **89**(3) 1159-1168 (1991).

Lamina thickness = 1.413 X 10^{-4} m.
Density = 1550 kg/m^3 Fiber volume = 60%
Q_{xx} = 145.5 GPa. Q_{xy} = 2.91 GPa Q_{yy} = 9.69 GPa Q_{ss} = 5.97 GPa

Table I Lamina properties of AS4/3502 graphite epoxy.

Laminate	Direction of Propagation	Measured Velocity (m/s)	Theoretical Velocity (m/s)
$[0_{16}]$	0	9020	9690
	45	3510	7004
	90	2700	2500
$[0_4,90_4]_s$	0	6380	7087
	45	5210	5469
	90	7300	7087
$[0,90]_{4s}$	0	6550	7087
	45	5020	5469
	90	6450	7087
$[0,45,-45,90]_{2s}$	0	6050	6321
	45	5990	6322
	90	5750	6321

Table II Measured and theoretical extensional velocities for AS4/3502 graphite/epoxy laminates.

Figure 1 Typical AE signal in thin plate identifying extensional and flexural plate modes.

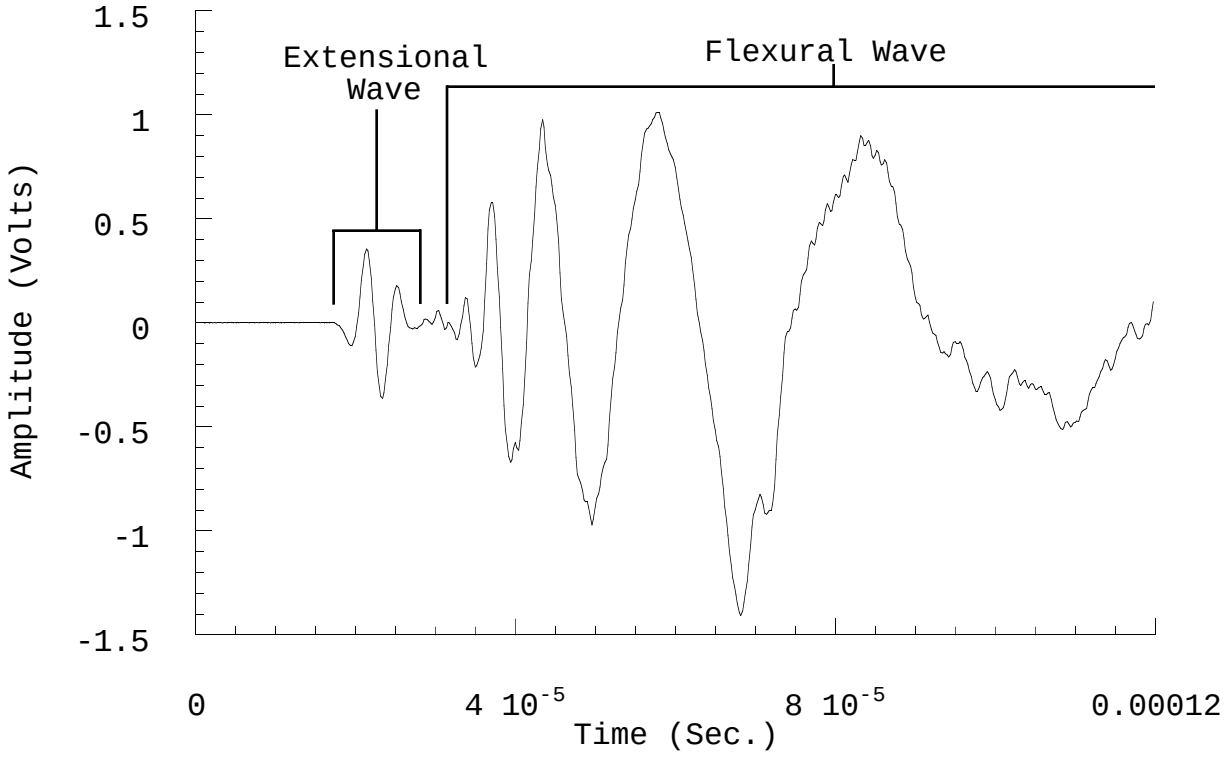

Figure 2 Plot of extensional arrival time versus distance of propagation for 90 degree propagation in $[0_{16}]$ graphite/epoxy plate.

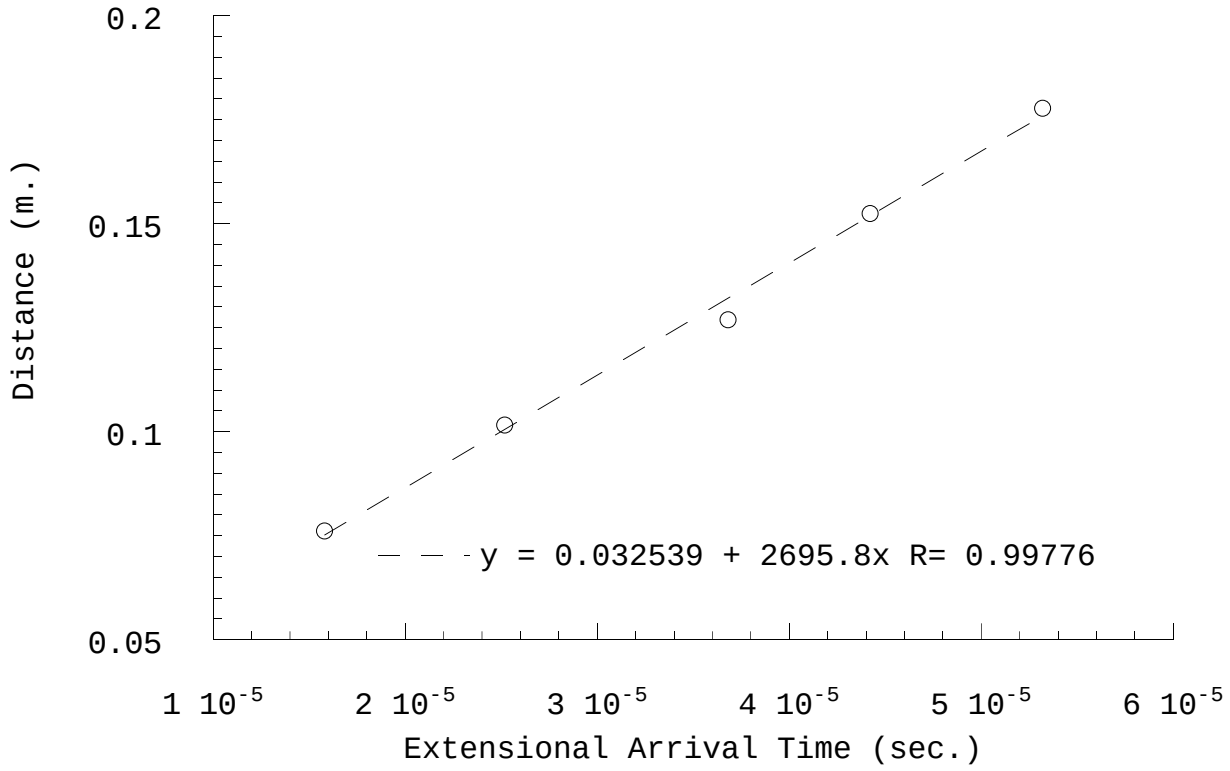

Figure 3 Experimental setup for flexural velocity measurements in composite plates.

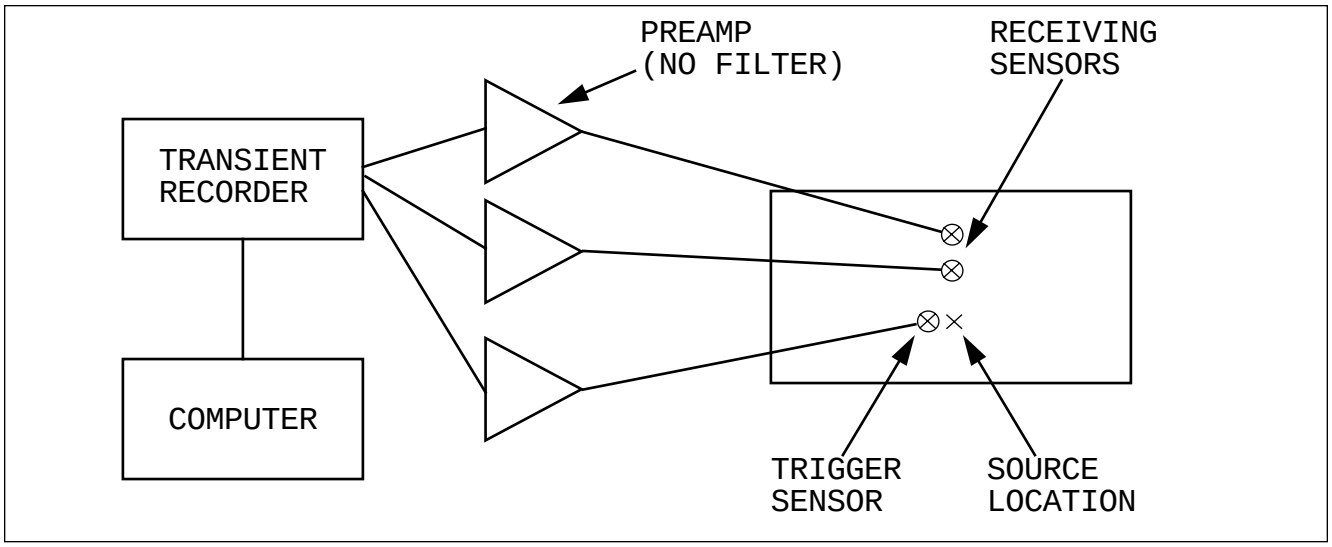

Figure 4 Measured and theoretical flexural dispersion for 0 degree propagation in $[0_{16}]$ graphite/epoxy plate.

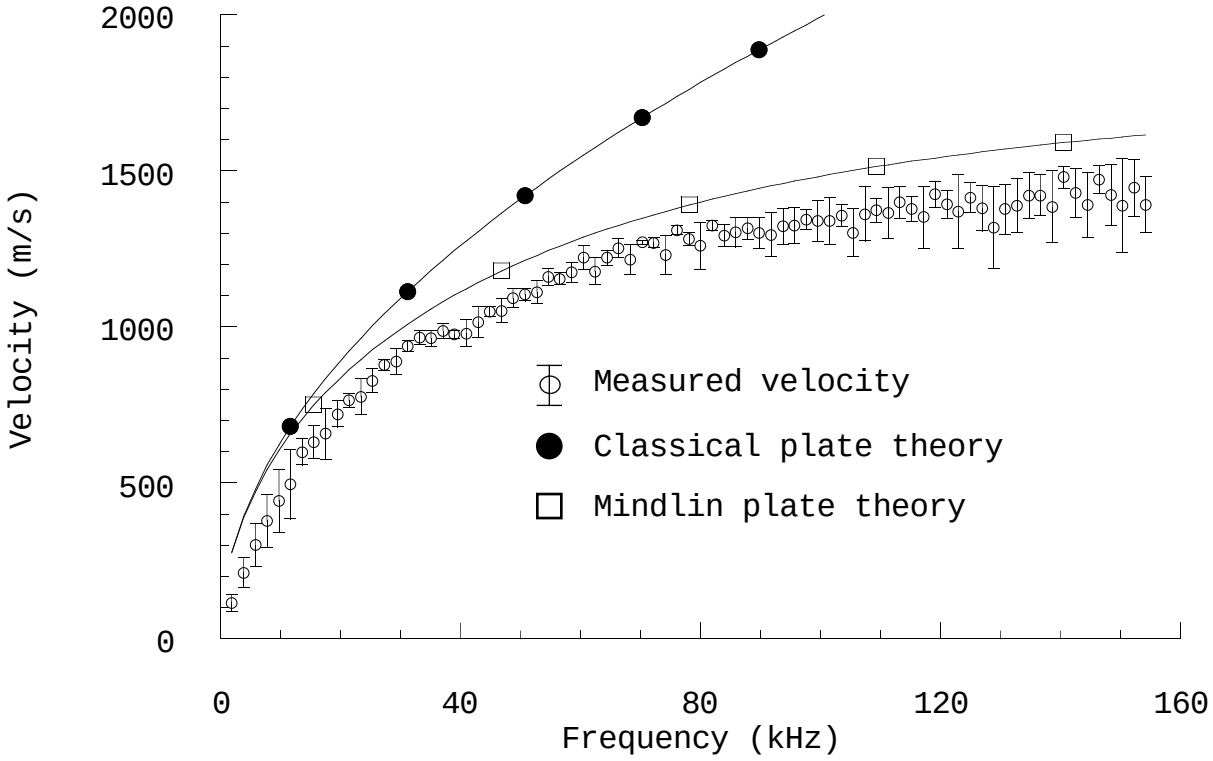

Figure 5 Measured and theoretical flexural dispersion for 45 degree propagation in $[0_{16}]$ graphite/epoxy plate.

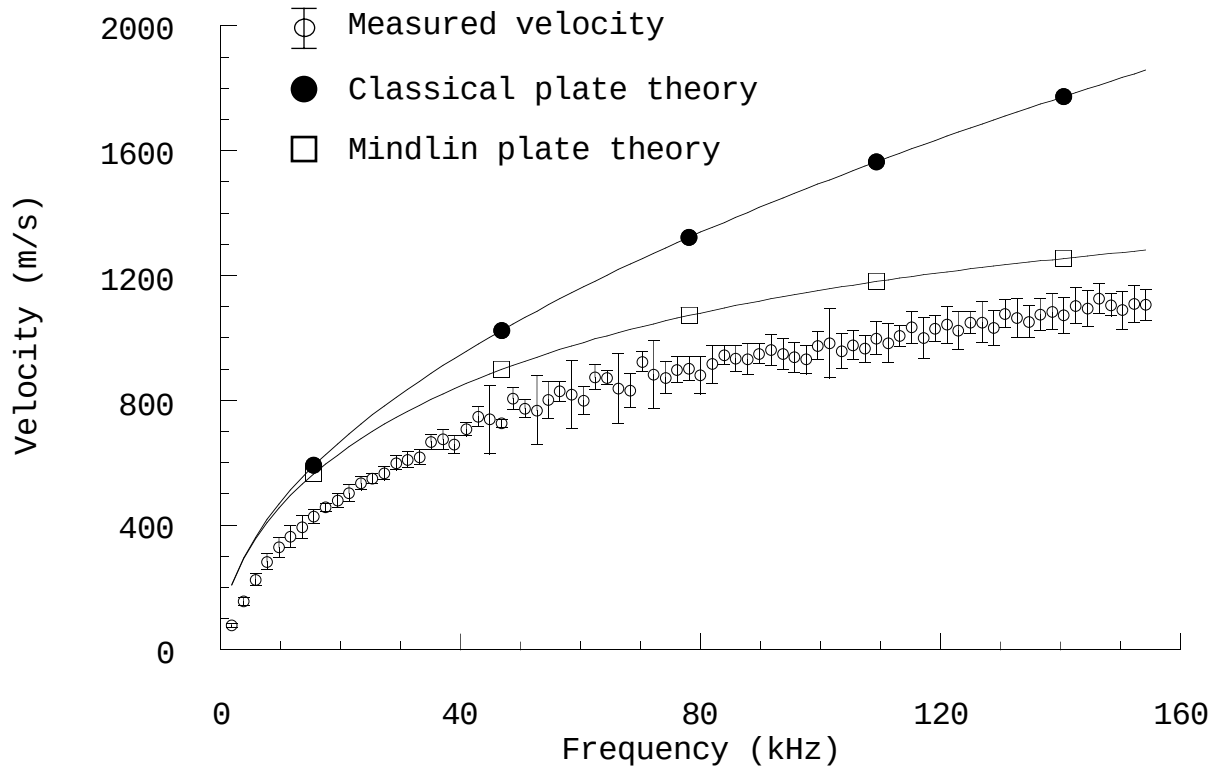

Figure 6 Measured and theoretical flexural dispersion for 90 degree propagation in $[0_{16}]$ graphite/epoxy plate.

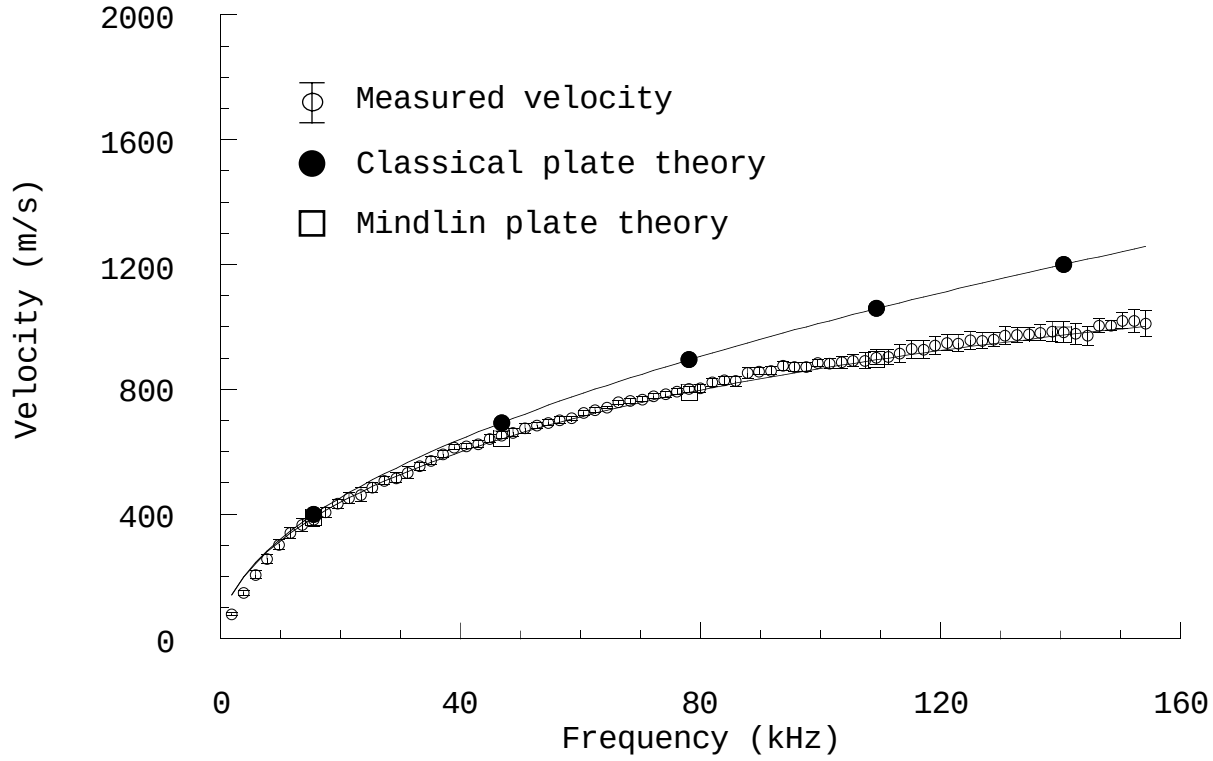

Figure 7 Measured and theoretical flexural dispersion for 0, 45, and 90 degree propagation directions in $[0,90]_{4s}$ graphite/epoxy plate.